ISFV13 - 13th International Symposium on Flow Visualization
FLUVISU12 - 12th French Congress on Visualization in Fluid Mechanics
July 1-4, 2008, Nice, France

PARTICLE-BASED VORTEX CORE LINE TRACKING TAKING INTO ACCOUNT VORTEX DYNAMICS

Tobias Schafhitzel*, Kudret Baysal, Ulrich Rist**, Daniel Weiskopf***, Thomas Ertl***
*Institute of Visualization and Interactive Systems, Universität Stuttgart
**Institue for Aerodynamics and Gasdynamics, Universität Stuttgart
***VISUS – Visualization Research Center, Universität Stuttgart**

KEYWORDS:
Main subject(s): *Flow Visualization, Vector Field Visualization*
Fluid: *...*
Visualization method(s): *Vortex Visualization, Segmentation,...*
Other keywords: *...*

ABSTRACT: *In this paper, we propose a framework which allows the tracking of segmented vortex structures taking into account vortex dynamics. Our framework is based on the work of Stegmaier et al.[SRE05], where the vortex core line of each vortex of a given flow is computed to provide a segmented representation. This work is extended as follows: (1) vortex tracking: the core lines are considered as connected particles which are integrated along a given time-dependent vector field and tested against overlapping with the core lines of the following time step; (2) consideration of vortex dynamics: during the tracking process of a selected vortex, and for each time step, the vortex with the highest impact, is computed; then the time step of the strongest perturbation t_p is determined; (3) tracking of the perturbing vortices: starting at t_p, the vortex structures with the highest impact are tracked to provide information about their spatiotemporal evolution; (4) visualization: vortical regions are represented by segmented λ_2 isosurfaces which are highlighted using color coding and bounding boxes in the case they are tracked. According to vortex dynamics, the individual degree of impact is determined by evaluating the Biot-Savart Equation for each vortex. Finally, the resulting vector field is used to compute the kinetic energy and the enstrophy respectively, which serves as a global value of influence over the whole perturbed vortex structure.*

1 Introduction

The investigation of coherent structures in time-dependent flow is one of the most important applications in the field of fluid dynamics. Thereby, the name *coherent structure* can be ascribed to the spatial and temporal coherence, which is required for the characterization of flow fields by the detection of organized structure motions. Particularly for the consideration of vortex dynamics, i.e., the interaction between different coherent structures, the temporal coherence plays a crucial role. The capability of identifying vortex structures and their time-dependent development would allow an advanced study of kinematic properties, e.g., size, shape, energy, enstrophy, strength as well as the origin, growth, dissipation and stability as dynamic properties of time-dependent flow fields [Adr07].
The process of tracing several vortex structures along time is called *vortex tracking*, and its

application reaches from basic research in fluid dynamics, e.g., for the comparison and validation of different simulation techniques, to the exploration of wind flows around vehicles in wind tunnels. Thereby one main concern of the engineers consists of the backward-tracking of critical vortices, e.g., vortices which might influence the driving behavior negatively, to gain information about their spatiotemporal evolution. Here, the interaction between different vortex structures is not negligible, as particularly strong, spatially close vortices are able to influence the motion of their neighborhood. Consequently, though it is possible to classify a vortex as critical at time t, the source of its criticality is not clear: either it could be the result of a negative impact of its neighbors, or the vortex generated at an unmeant location, or it could be a combination of both.
The goal of this work consists of the detection of perturbation events on arbitrary temporarily tracked vortex structures. Starting with a segmented representation of the individual vortices, the vorticity inside each structure serves as input for the Biot-Savart equation, which computes the velocity induced from one vortex structure to another. In order to compute a global value, which represents the influence of a neighboring vortex to the entire domain selected by the user, i.e., a selected vortex structure, two different quantities are taken into account: the kinetic energy and the enstrophy. Both quantities are computed on the induced velocity field and its respective derivatives. Once the impact of each vortex to a selected structure is computed, the time of the highest perturbation is determined. This time serves as the starting point of a new tracking process, which considers, in contrast to the previous vortex tracking, the critical vortex, i.e., the vortex with the highest impact as well as the selected vortex structure. This leads to a clear identification of critical perturbation events to an arbitrary vortex structure. The results of this computation are visualized within a graphical framework, which provides the user full interaction in terms of selecting several vortex structures to explore their temporal behavior, and in particular, to gain information about their location and time of generation. In addition, the user is able to find out the time at which the selected vortex is perturbed massively by another vortex, and finally, to see where this critical vortex is coming from.

2 Previous Work

The pioneering works in analysis of vortex structures in order to investigate flow fields were done by Theodorsen [The52]. The fundamental innovation of Theodorsen was the detection of so-called hairpin-like vortex structures and the importance of this structures for generation, conservation and spreading of turbulence. The detection of the hairpin-like vortex structures led to several approaches for turbulence models based on vortex structures [AS87], [Adr07], [CBA05], [PC82], [The52]. However, the acceptance of this turbulence models was limited due to the fact that the vortex structures described by Theodorsen were not verifiable by experiments, caused by the limitations of experimental methods and the complexity of the structures. Only the improvements in experimental methods [HB81] led to a clear verification of the hairpin-like vortex structures and to a broader acceptance of the turbulence models based on the work of Theodorsen. An enhancement of the single hairpin-like vortex structures was proposed by Adrian et al. [AMT00]. In this approach, packages of hairpin-like vortices are considered, which are created in terms of an auto-generation process. In previous work, the investigation of auto-generation is done by a pure visualization of vortex structures (experiments or isosurface visualization of miscellaneous values in numerical results). The tools approached in this paper enable a more detailed investigation of the

dynamical mechanism of the structures.
The vortex core line is defined as the geometrical and dynamical simplification of a three dimensional vortical region to a line. To the author's knowledge there exists no unique definition of a vortex core line; most of recent work bases on the assumption, that the pressure behaves minimal along the vortex core line. Banks and Singer [BS95] proposed a predictor-corrector algorithm using the pressure and the vorticity for the identification of the core line. This method was extended by Stegmaier et al. [SRE05] by replacing the pressure by the Galilean-invariant λ_2 quantity introduced by Jeong and Hussain [JH95]. Peikert reformulated most of recent vortex core line detection methods using the parallel vectors operator [PR99]. Adopting the concept of feature flow fields [TS03], the parallel-vectors operator can be used to trace ridge and valley lines of local criteria like λ_2 from local extremum points [SWH05]. This idea can be extended to track core lines over time [TSW$^+$05]. Recently, Weinkauf et al. [WSTH07] have extended this class of algorithms by proposing the coplanar-vectors operator, which is applied for the extraction of cores of swirling particle motion in transient flows.

3 Theoretical Basics on Vortices

In this section, a short introduction to the definition of vortical regions, the computation of vortex core lines and vortex dynamics is given.

3.1 λ_2 Vortex Criterion

In recent research there exist various approaches for the identification of vortical regions [KM98, CQB99, DD00, JH95, WXY05]. One of the most effective methods consists of the λ_2 method [JH95], which is based on the assumption of local pressure minima inside vortex structures. However, the computation of λ_2 depends on the velocity gradient tensor, what makes the method *Galilean Invariant*. For a more detailed description, we refer to the work of Jeong et al. [JH95]. The governing equation for the λ_2 method is

$$\frac{DS_{ij}}{Dt} - \nu S_{ij,kk} + \Omega_{ik}\Omega_{kj} + S_{ik}S_{kj} = -\frac{1}{\rho}p_{i,j}, \tag{1}$$

where ρ represents the pressure and S and Ω denote the symmetric and antisymmetric part of the velocity gradient tensor, respectively. The first two terms on the left hand side are neglected in order to consider the inconsistency between the existence of a pressure minimum and the existence of a vortex. In the following, a brief description of the λ_2 method is given: Let $\mathbf{v}(\mathbf{x}) = (v_x, v_y, v_z)^T$ be a 3D vector field. Then, the velocity gradient tensor or Jacobian is defined as $J = \nabla\mathbf{v}$. By the decomposition of this matrix into a symmetric and an antisymmetric part, the strain-rate tensor and the rotation tensor are obtained. The strain-rate tensor is defined by

$$S = \frac{1}{2}(J + J^T) \quad with \quad S_{i,j} = \frac{1}{2}\left(\frac{\partial v_i}{\partial x_j} + \frac{\partial v_j}{\partial x_i}\right), \tag{2}$$

and the rotation tensor by

$$\Omega = \frac{1}{2}(J - J^T) \quad with \quad \Omega_{i,j} = \frac{1}{2}\left(\frac{\partial v_i}{\partial x_j} - \frac{\partial v_j}{\partial x_i}\right), \tag{3}$$

respectively. In order to compute the vortex strength, namely the λ_2 value for a point inside the flow, the matrix $M = S^2 + \Omega^2$ is constructed. The tensor M is the *corrected Hessian of pressure* (see equation 1). Due to the fact that M is real and symmetric, it has exactly three real eigenvalues, which can be sorted according to $\lambda_1 \geq \lambda_2 \geq \lambda_3$. The value for the λ_2 vortex criterion is identical to the above eigenvalue λ_2.
Actually, vortex regions are defined as regions where $\lambda_2 < 0$, i.e., vortex boundaries are given by isosurfaces of λ_2 with isovalue 0. Decreasing, negative λ_2 values correspond to increasing vortex strength. Therefore, vortices are often extracted by isovalues less than 0 in order to remove weak vortices.

3.2 Vortex Core Lines

The motivation of vortex core lines consists of the geometrical reduction of a vortical region to a line. Each vortical region detected by the λ_2 criterion is supposed to have a rotation axis. This axis, called vortex core line, can be defined as the connection of local pressure minima, and according to Stegmaier et al. [SRE05], as a connection of local λ_2 minima.
Our definition of vortex core lines is similar to the definition of valley lines on the λ_2 scalar field. Therefore, each point on the valley line underlies a number of restrictions: let us start with a 3D non-degenerate λ_2 minimum, i.e., a point with a vanishing gradient $\nabla\lambda_2(\mathbf{x}) = \mathbf{0}$ and three positive eigenvalues of its Hessian $\mathscr{H}\lambda_2$, which is a real symmetric matrix. The definition of valley lines relaxes these conditions, i.e., a point on the valley line is required to be a minimum perpendicular to its gradient, but in contrast to a 3D minimum, the λ_2 value along the valley line should be allowed to vary. This means, that a point on the valley line is defined to be a minimum in all directions except for the direction of the lowest or a negative change. Let $\eta_0 \geq \eta_1 \geq \eta_2$ be the eigenvalues and $\varepsilon_0, \varepsilon_1, \varepsilon_2$ the respective eigenvectors of the Hessian at a point $\mathbf{x}$. Then, $\lambda_2(\mathbf{x})$ is a minimum on the plane spanned by ε_0 and ε_1 when $\eta_1 > 0$. Peikert et al. [PR99] reformulated this problem using the parallel vectors operator with $\nabla\lambda_2 || \nabla(\nabla\lambda_2) \cdot \nabla\lambda_2$, stating that the gradient of λ_2 needs to be linearly dependent on the second order derivative of λ_2 along the gradient.
Note, that following the definition above, the gradient of the valley line is collinear to ε_2. However, this requires the computation of the second order derivatives and its eigenvectors of λ_2, what might lead to inaccuracies due to noise. Both the predictor corrector methods of Banks and Singer [BS95] and Stegmaier et al. [SRE05] used the vorticity as an appropriate approximation of ε_2. In this paper, we follow the method of Stegmaier et al. to compute the vortex core lines.

3.3 Vortex Dynamics

The consideration of vortex dynamics enables a more detailed insight into the temporal behavior of coherent structures. In detail, vortex dynamics connect the evolution and interaction of coherent structures to their topology. A simple method for the consideration of vortex dynamics consists of the analysis of dynamical values, e.g., kinetic energy or enstrophy:

$$E_{kin} = \frac{1}{2} \int \int \int_V \rho \left(\mathbf{v}(\mathbf{x},t)\right)^2 dV, \tag{4}$$

$$E_{rot} = \frac{1}{2} \int \int \int_V \omega(\mathbf{x},t)^2 dV. \tag{5}$$

Thereby, the problem consists the definition of the region of integration. In designed cases with two vortex structures like collision of vortex rings [KT94], it is sufficient to integrate over the whole domain. In real flow fields containing hundreds of structures of interest, each of them needs a more specified definition of the integrated volume. A reasonable choice are the spatial extensions of the vortical regions.
Another technique consists of the investigation of the interactions between vortex structures and other flow features, e.g., shear layers or other vortices. Particularly the interaction between vortex structures is rather important, e.g., in 2d vortex merging [JR07] and in 3d collision of vortex rings [KT94]. The information obtained by identification, segmentation and tracking of vortex structures allows an intensified study of the interaction between several vortex structures. The fundamental equation for the analysis of vortex dynamics is the Biot-Savart equation 6, which computes the induced velocity field out of the vorticity:

$$\mathbf{v}_{ind}(\mathbf{x},t) = \frac{1}{4\pi}\int\int\int_{\mathbf{x}} \frac{\omega(\mathbf{x}',t)\times(\mathbf{x}-\mathbf{x}')}{|\mathbf{x}-\mathbf{x}'|^3} d\mathbf{x}'. \tag{6}$$

In general, a velocity field can be represented as the sum of rotational and irrotational parts. The irrotational part is determined by the boundary condition. The rotational velocity, denoted as v_{ind} in equation 6, is completely determined by the vorticity field.
By the computation of the velocity induced by the vorticity field of a single vortex structure S_1, the influence of this structure on its environment is determined. Considering the environment, if the kinetic energy or the enstrophy is computed only of the induced velocity inside one vortex structure S_2, the results allow a quantitative estimation of the influence of S_1 to S_2.

4 Vortex Tracking taking into Account Vortex Dynamics

In this section, the tracking process is discussed, beginning with the detection of vortical regions, followed by the tracking of the vortex core lines to the consideration of vortex dynamics. The visualization of the results is discussed later in section 5.

4.1 Vortex Core Line Detection

Since our vortex core line detection method bases on the implementation of Stegmaier et al. [SRE05], only a brief description is given. Based on the given velocity field, first the λ_2 scalar field and the vorticity vector field are computed to use them as input for the skeleton growing algorithm. Starting at a 3D minimum of λ_2 at position p_0, the skeleton grows in the direction of the vorticity vector and its opposite direction. After each integration step, a plane $\mathscr{P}$ perpendicular to the vorticity vector at the new position p_1' is computed to search the minimum λ_2 value on it. This correction step determines the next position p_1 on the vortex core line, which is supposed to be a minimum on $\mathscr{P}$ (see 3.2). These two steps are repeated for each 3D minimum until one of the exit conditions, e.g., the exceed of the isovalue of the covering λ_2 hull, is fulfilled. Keep in mind, that the isosurface serves as spatial border for the growing vortex core line, and therefore, the λ_2 isovalue should be chosen nearby 0.

4.2 Vortex Core Line Tracking

Once the vortex core lines and their respective λ_2 isosurfaces are computed for each time step, we need to assign the structures at time t to their corresponding structures at time $t+1$.

This mapping process is called *tracking* and depends directly on the given velocity field. However, the tracking of geometrical structures, particularly isosurfaces covering vortical regions, requires a more detailed consideration: let us consider a particle at an arbitrary position inside a vortical region, i.e., according to section 4.1 it is covered by a λ_2 isosurface. Then, its motion strongly depends on the selected reference frame: in the first case, the reference frame moves along with the vortex structure; in the second case, a static reference frame is used. While in the first case the motion of the particle is observed as a pure rotation, the same particle describes a convection in the static reference frame. Since our method uses a static reference frame, the motion of the particle consists of the vortex structure's motion and the rotation around the vortex axis. Therefore, for the tracking of whole structures the rotation needs to be disregarded.
The only spatial region which guarantees a particle's motion without the rotation around the vortex axis, is the vortex axis itself. Furthermore, placing the particles on the core line provides an appropriate sampling of the structure. This is due to the definition of the vortex core line, namely the connection of local λ_2 minima, which is expected, because of the temporal smooth behavior of λ_2, to change least from one to the next time step (see 3.2).
The tracking works, similar to the vortex core line detection, in a predictor-corrector manner. In order to track a vortical region, the vortex core line is sampled, whereas for each sample point a particle is integrated along the velocity field. Once the new position p'_{t+1} is computed, the nearest structure p_{t+1} is determined. This is done by measuring the particle's euclidian distance to the several vortex core lines. Furthermore, the particles are tested if they are located inside the core line's λ_2 isosurface. Here, each vortex structure has its own counter which holds the number of particle hits and the respective *source vortex* id from where the particles were emitted. Keep in mind, that the corrected positions are used for further tracking.
Although it is expected, that most of the particles hit the same structure at $t+1$, it might happen, that more than one structure were hit by particles holding the same source vortex id. This event can be ascribed to the topological changes of a vortex structure along the time. For example, a vortex can be split or merged with another vortex structure [KT94]. Keep in mind, that the correctness of the topological changes depends strongly on the underlying vortex core line detection method. Though the method of Stegmaier et al. [SRE05] provides a high quality of the detected core lines, it is not guaranteed that all actually connected structures are detected as connected.
To the author's knowledge, there exists no recent work guarantying the topological correctness of vortex core lines. We solve this issue by taking into account all vortex structures which are hit by any particles, except for the vortex structures which are hit by a relatively small number of particles with respect to the number of emitted particles or the length of the vortex hit by the particles. This prevents of an unmeant discard of possibly important vortex structures and is expressed by the following two conditions which must be fulfilled:

$$\frac{n_i^{[t]}}{n_o^{[t]}} \geq a \quad and \quad \frac{n_i^{[t]}}{n_o^{[t-1]}} \geq b, \tag{7}$$

where $n_i^{[t]}$ stands for the number of incoming particles and $n_o^{[t]}$ for the outgoing particles, respectively. The first condition claims that a structure was hit by at least a times its length, the second condition ensures, that an appropriate number of emitted particles hit the current structure. In our implementation we obtained the best results by setting both ratios to $5 \sim$

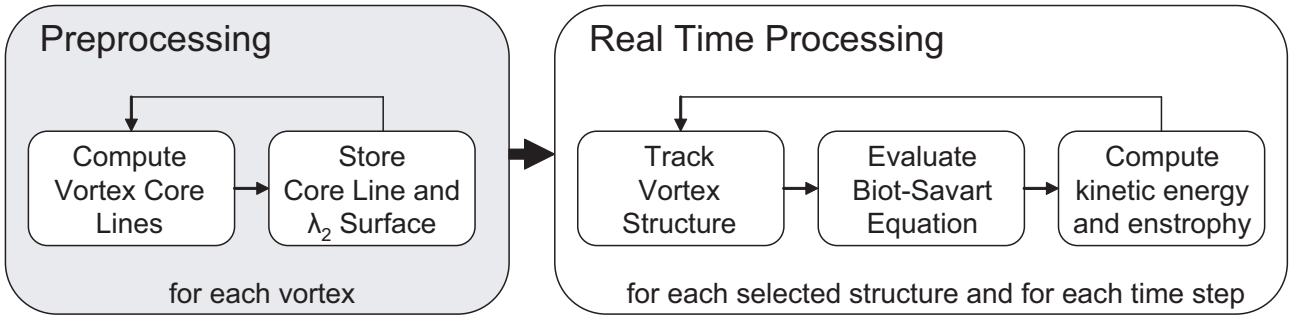

Figure 1 Program flow of our framework: in the first stage the vortex core lines are computed in order to segment the vortex structures according to the λ_2 criterion. All the pre-computed structures are stored to provide a fast access during the second stage. In this stage, the structures are tracked and computed for their influence to each other. This stage can be interactively manipulated by the selection of the structures to be tracked.

10%. Once a vortex is hit, its id is added to a list holding all the necessary information which is used for further tracking.

4.3 Vortex Dynamics

By applying the vortex core line detection and the tracking of the resulting structures as described above, the user is able to select and explore the temporal behavior of any vortical regions. In this section, we introduce the consideration of vortex dynamics during the tracking process, i.e., the way different vortex structures influence each other. This extends our algorithm in a way, the tracked vortex structures are investigated spatiotemporally.
The influence of one vortex structure to another is described by a single scalar value: the kinetic energy and the enstrophy, respectively. Both quantities depend on a given velocity field which need to be computed first. For this purpose, the Biot-Savart equation is evaluated as described in section 3.3 using the segmented λ_2 isosurfaces as an appropriate representation of vortex structures. In our implementation, each vortex holds a pointer to a discreet grid containing the positions inside the structure which can be used to access and store the vorticity and the induced velocity field, respectively. This makes the evaluation of equation 6 rather simple. For each cell inside the destination vortex, we integrate over all cells of the source vortex to sum up their distance weighted vorticity. The algorithm finishes when each of the destination cells is filled with a velocity vector.
In the next step, the resulting velocity field is used to compute the kinetic energy as well as the enstrophy induced by the source vortex. In contrast to the kinetic energy, the enstrophy depends on the vorticity $\nabla \times \mathbf{v}_{ind}$ induced, what makes it necessary to compute the partial derivatives of the induced velocity field first. Our internal structure representing the induced velocity field allows us to use finite differences. Both quantities are computed according to equation 4 for the kinetic energy and 5 for the enstrophy. Since most of our data is measured or simulated in pure air, the density ρ is set to $1.2051 kg/m^3$ (air at $20\,^{\circ}\mathrm{C}$).
Figure 1 shows the overall program flow which is separated into two independent parts: the preprocessing, where the core lines and the vortex segmentation is computed, and the real time processing which consists of the tracking and the consideration of vortex dynamics. In contrast to the first stage, the second stage can be widely influenced by the user.

Though algorithm 1 only considers the enstrophy, the computation of the kinetic energy follows the same scheme. Although, for the sake of simplicity, this example assumes the vortex structure to be selected at time $t = 0$, our implementation allows the selection of an arbitrary vortex structure at any time t. Note, that due to topological changes along the time, the variable *selectedVortex* may consist of more than one structure. In the first loop, all vortex structures are considered, except for the selected structure, to compute their influence on it. After the evaluation of the Biot-Savart equation, the enstrophy is computed and stored in the case it has the maximum influence. The variable *selectedVortex* represents the id of the selected vortex at any time. Once the strongest items, i.e., the items with the highest impact, are computed for each time step, the overall maximum perturbation is obtained by comparing the results of the different time steps. Then, the tracking is started again at time t_p, the time of the strongest perturbation, to deliver a representation in which the impacted vortex as well as the strongest source of perturbation are included. This plays a crucial role for the following visualization of the results.

5 Visualization of the Results

The last stage of processing time dependent vector fields for the investigation of vortical structures consists of the visualization. Although the goal of our visualization consists of the representation of the vortex with the strongest influence to a user selected structure, the framework provides a variety of opportunities for the more detailed exploration of vortical structures. According to [SRE05], all vortices are represented as λ_2 isosurfaces and their corresponding vortex core lines. All geometrical primitives are stored in a scene graph which allows the selection of single structures, either to explore them in more detail or for fading

Algorithm 1 Vortex Tracking taking into account enstrophy.

```
void getstrongestPerturbation(id selectedVortex)
{
for t=minTime to maxTime        // loop over all time steps
   for i=firstVortex to lastVortex // loop over all vortices except for the selected one
      indvel[] = BiotSavart( i, selectedVortex);
      float en = computeEnstrophy(getVorticity(indvel));
      if max(en)
        setStrongestVortex(i, t);
      endif
   endfor
   trackStructures( selectedVortex, t+1);
endfor
// get the strongest Vortex and the time of strongest perturbation
getStrongestPerturbation( strongestVortex, t_p);
selectedVortex = getSelectedVortexAtTime(t_p);
trackIDs[] = strongestVortex + selectedVortex;
for t=t_p to timeMin // then track all the structures
   trackStructures(trackIDs, t-1);
endfor
for t=t_p to timeMax
   trackStructures(trackIDs, t+1);
endfor
}
```

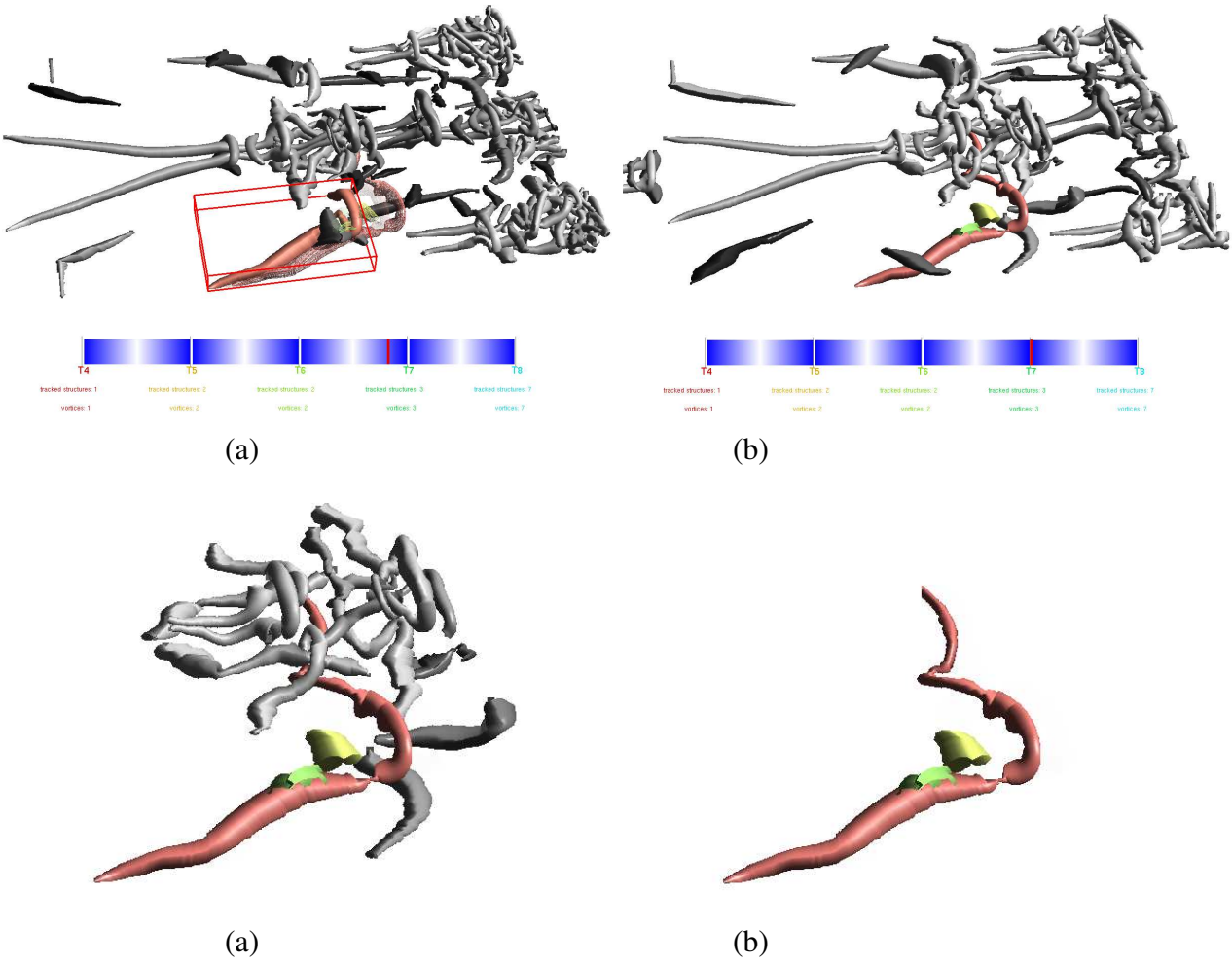

Figure 2 A simulation of a transition on a flat plate. The flow moves from left to the right. In this example only the tracking of vortical regions is illustrated: (a) a vortex structure is selected for tracking at an arbitrary time, here $t = 4$. The wire frame representation shows the motion of the vortex; (b) the context is switched to a particular time of interest; (c) due to the underlying scene graph the context can be scaled down; (d) only the tracked vortex structure is displayed. The other vortex structures created due to temporal split events are clearly perceptible.

them out or, last but not least, to select them for tracking. Figure 3(a) shows such an initial situation: the visualization of all detected vortex structures to a specific time, color coded according to their strength. Here, the color gradient goes from green (weak) to red (strong). Once a vortex has been selected, the tracking process is ready for execution. Thereby, it plays no role to which time the tracking is started, because the particle integration is applied along the positive and the negative time. Keep in mind, that starting the tracking of a specific structure at different times might lead to different results. This is due to the topological changes, e.g., if the tracking of the structure is started at $t = 0$, all the structures which are created as a consequence of split events are considered additionally for further tracking, while they remain unconsidered if the tracking of the same structure is started at a later time. Nevertheless, this behavior is correct regarding that only structures are taken into account which are directly selected by the user.

The representation of the vortices follows a focus and context scheme, where the vortex

structures of the initial time build the context while the focus lies on the tracked structure. Figure 2(a) illustrates this case. The representation of the tracked structures is also user defined, whereby the position of the mouse cursor on a time line decides which structure has to be drawn. The time line also provides the fading between two consecutive time steps. This representation allows the user a fast identification of spatial and temporal events of interest, and therefore, once a time step is identified as of particular interest, the context can be switched to represent the vortex field at the selected time (Figure 2(b)). For further investigation, the advantages given by the scene graph can be exploited: uninteresting structures are faded out, in order to scale down the context (Figure 2(c)) or only the single tracked vortex structure is explored (Figure 2(d)). The sequence in Figure 2 also shows the occurrence of vortex split events, where the several parts are perceptible at a glance supported by color coding. Keep in mind, that these structures are all considered for further tracking.
The next example extends the tracking method by taking into account vortex dynamics in order to find the time where the selected structure is perturbed strongest by another vortex. The computation results in a list containing the strongest perturbing vortices and the appropriate information in terms of kinetic energy and enstrophy, respectively. The results can be visualized with respect to both quantities, whereas the user is able to switch between both representations.
The resulting time t_p defines the time of the strongest perturbation, and therefore, the visualization is set to t_p for both the focus and the context. In Figure 3, the detection and visualization of t_p is shown. By selecting a vortex at an arbitrary time (Figure 3(a)), the vortex with the strongest influence is computed, displayed as green vortex in Figure 3(b) at time t_p. Starting from here, both structures are tracked forward and backward to gain information about their origin and their further development (Figures 3(c) and (d)). Additionally, the detailed information about the detected and the selected vortex, e.g., the energy induced, ids, length etc. is displayed as text.

6 Conclusions and Future Work

The investigation of the temporal evolution of coherent structures is of high importance in order to understand the behavior of time dependent flows. For this purpose, we have developed a framework which allows the tracking of segmented vortex structures. Additionally, the interaction between the different vortices is taken into account by computing the induced velocity from one structure to another. The degree of impact is expressed by the kinetic energy and the enstrophy, respectively. The method proposed allows the user to explore a selected vortex structure for its temporal and spatial evolution and to detect the strongest perturbing vortex structure as well as its corresponding time of impact.
In the future, the mechanism can be applied in an inverse manner, i.e., the structure which is perturbed strongest by a selected vortex can be determined. Furthermore, the degree of self-influence can be taken into account by considering the induced velocity of a vortex structure to itself. Last but not least, other structures can be considered for their contribution to the induced velocity inside vortical regions. An example would consist of shear layers.

7 Acknowledgements

We would like to thank Fulvio Scarano (Technische Universiteit Delft) for providing the experimental data set showed in Figure 3 and Daniel Meyer (Universität Stuttgart) for the simulated

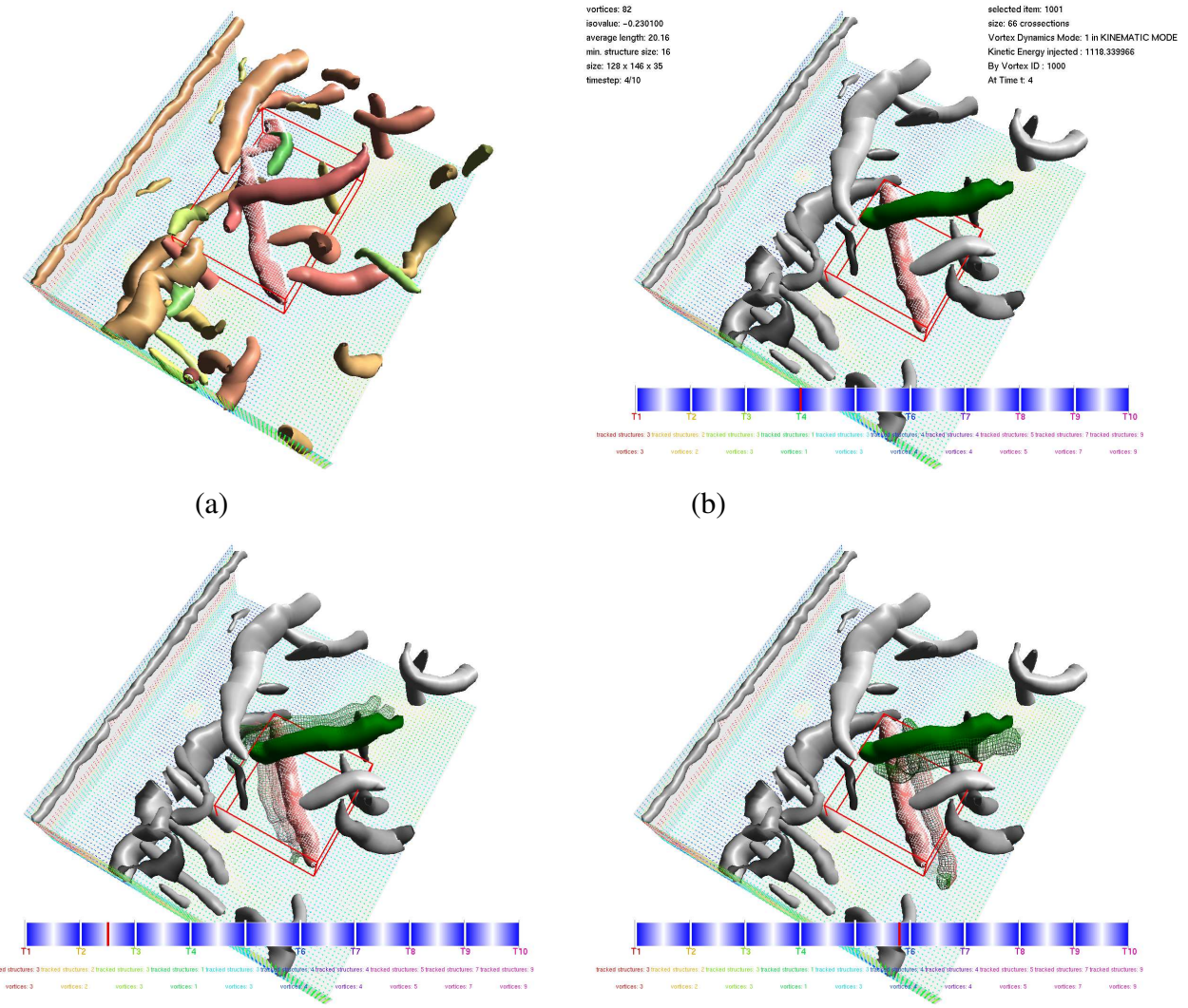

Figure 3 The visualization of an experimental data set. The data was measured using tomographic PIV and shows a circular cylinder wake at Reynolds $Re = 360$. The cylinder, which is located parallel to the left edge of the data set is not visualized. In this example, vortex dynamics are considered: (a) initial situation at $t = 0$. All vortices are color coded according to their strength. The red bounding box gives feedback about the vortex selected for tracking; (b) the moment of strongest perturbation at $t_p = 4$. The representation has changed to time t_p where the green vortex influences the selected structure (red); (c) backward tracking. The wire frame representation shows where the structures came from; (d) forward tracking. Here, the wire frame representation shows the further development of both structures.

data set used in Figure 2.

References

[Adr07] R. Adrian. *Hairpin vortex organization in wall turbulence*. Physics of Fluids, 19:041301, 2007.

[AMT00] R. Adrian, C. Meinhart and C. Tomkins. *Vortex organization in the outer region of the turbulent boundary layer*. J. Fluid Mech., 422:1–54, 2000.

[AS87] M. Acarlar and C. Smith. *A study of hairpin vortices in a laminar boundary layer. part 2.* J. Fluid Mech., 175:43–83, 1987.

[BS95] D. C. Banks and B. A. Singer. *A predictor-corrector technique for visualizing unsteady flow*. IEEE Transactions on Visualization and Computer Graphics, 1(2):151–163, 1995.

[CBA05] P. Chakraborty, S. Balachandar and R. Adrian. *On the relationships between local vortex identification schemes*. J. Fluid Mech., 535:189–214, 2005.

[CQB99] R. Cucitore, M. Quadrio and A. Baron. *On the effectiveness and limitations on local criteria for the identification of a vortex*. European Journal of Mechanics - B/Fluids, 18(2):261–282, 1999.

[DD00] Y. Dubief and F. Delacayre. *On coherent-vortex identification in turbulence*. Journal of Turbulence, 1(11):10.1088/1468–5248/1/1/011, 2000.

[HB81] M. Head and P. Bandyopadhyay. *New aspects of turbulent boundary layer structure*. J. Fluid Mech., 107:397–338, 1981.

[JH95] J. Jeong and F. Hussain. *On the identification of a vortex*. Journal of Fluid Mechanics, 285:69–94, 1995.

[JR07] C. Josserand and M. Rossi. *The merging of two co-rotating vortices: a numerical study*. European Journal of Mechanics B/Fluids, 26:779–794, 2007.

[KM98] S. Kida and H. Miura. *Identification and analysis of vortical structures*. European Journal of Mechanics - B/Fluids, 17(4):471–488, 1998.

[KT94] S. Kida and M. Takaoka. *Vortex reconnection*. Annu. Rev. Fluid Mech., 26:169–189, 1994.

[PC82] A. Perry and M. Chong. *On the mechanism of wall turbulenc*. J. Fluid Mech., 119:173–217, 1982.

[PR99] R. Peikert and M. Roth. *The 'Parallel Vectors' Operator – A Vector Field Visualization Primitive*. In: Proceedings of IEEE Visualization '99, pp. 263–270, 1999.

[SRE05] S. Stegmaier, U. Rist and T. Ertl. *Opening the Can of Worms: An Exploration Tool for Vortical Flows*. In: Proceedings of IEEE Visualization '05, pp. 463–470, 2005.

[SWH05] J. Sahner, T. Weinkauf and H.-C. Hege. *Galilean invariant extraction and iconic representation of vortex core lines*. In: Proc. EG / IEEE VGTC Symposium on Visualization (Eurovis), pp. 151–160, 2005.

[The52] T. Theodorsen. *Mechanism of turbulence*. In: Proc. of the 2nd Midwestern Conference on Fluid Mechanics, pp. 1–19, 1952.

[TS03] H. Theisel and H.-P. Seidel. *Feature flow fields*. In: Proc. EG / IEEE TCVG Symposium on Visualization '03, pp. 141–148, 2003.

[TSW+05] H. Theisel, J. Sahner, T. Weinkauf, H.-C. Hege and H.-P. Seidel. *Extraction of parallel vector surfaces in 3D time-dependent fields and application to vortex core line tracking*. In: Proc. IEEE Visualization '05, pp. 631–638, 2005.

[WSTH07] T. Weinkauf, J. Sahner, H. Theisel and H.-C. Hege. *Cores of swirling particle motion in unsteady flows*. IEEE Transactions on Visualization and Computer Graphics (Proceedings Visualization 2007), 13(6):1759–1766, 2007.

[WXY05] J.-Z. Wu, A.-K. Xiong and Y.-T. Yang. *Axial stretching and vortex definition*. Physics of Fluids, 17:038108, 2005.

Copyright Statement